

# A bonnet and fluid jet polishing facility for optics fabrication related to the E-ELT

G. Vecchi, S. Basso, M. Civitani, M. Ghigo, G. Pareschi, M. Riva, and F. M. Zerbi

Istituto Nazionale di Astrofisica – Osservatorio Astronomico di Brera, Via E. Bianchi 46,  
I-23807 Merate, Italy, e-mail: gabriele.vecchi@brera.inaf.it

**Abstract.** A robotic polishing machine has been implemented at INAF-Brera Astronomical Observatory within the T-REX project. The facility, IRP1200 by Zeeko Ltd., consists of a 7-axis computer-controlled polishing/forming machine capable of producing precision surfaces on several optical materials. The machine enables two methods, the bonnet and the fluid jet polishing. We report on the results of the standard bonnet polishing machine acceptance tests that have been completed at our site. We intend to use the machine to support development and production programs related to the European Extremely Large Telescope (E-ELT), in particular, for making part of the optics of the Multi-conjugate Adaptive Optics RelaY (MAORY) module.

**Key words.** Optical polishing – Polishing machines – Ultra-precision polishing

## 1. Introduction

The T-REX project has enabled to strengthen our labs with the aim to support R&D and production programs of the optics for the E-ELT, featuring aspheric surfaces exceeding 1-*m* in size. To this purpose, we have upgraded the Ion Beam Figuring (IBF) system described by Ghigo et al. (2014) and we have implemented the polishing facility described hereafter. We have acquired the 1200 model of the IRP (Intelligent Robotic Polisher) series machine made by Zeeko Ltd. in UK. The polishing machine is constituted of a base and bridge epoxy granite composite structures providing good vibration damping and thermal stability. The overall footprint is about 4.3*m* × 4.3*m* × 3*m*, including the machine itself plus the console, a chiller unit and the Slurry Management Unit (SMU). The largest manufacturable part is ≈1200 mm in size and the load capacity is

≈500 kg. The facility has been installed into a clean room of class ISO7 and ≈50 m<sup>2</sup> size, as shown in Fig. 1. The clean room has been built to guarantee that high value optical components, like those required by the E-ELT, will be manufactured in a controlled environment.

The baseline design of the E-ELT includes a 39-*m* diameter elliptic concave primary mirror (M1) (Cayrel 2012). M1 is composed of 798 quasi-hexagonal segments, ≈1.45 m corner to corner, made of low expansion glass or glass-ceramics. The conjunction of high volume manufacturing and tight tolerances on the surface accuracy of the off-axis aspheric segments represents a big challenge, but also an opportunity, that the European optics community and industry are facing. The MAORY module will be part of the first light instrumentation of the E-ELT, and it has been designed to correct for the atmospheric turbulence ef-



**Fig. 1.** The IRP1200 series machine in the clean room. The SMU is on the side of the machine, on the left. The SMU feeds the polishing process with recirculating pumped slurry maintained at constant temperature. An integrated density sensor monitors the specific gravity of the slurry.

fects on a wide field of view in the near infrared (Diolaiti et al. 2014). It will feature several mirrors and lenses that will have also to be manufactured to the ultimate form accuracy and quality standards.

## 2. The 7-axis robotic system

The distinctive process relies on a sub-aperture tool that polishes the surface and corrects its form while it is going along the workpiece by following a defined path. To this purpose, the relative motion and orientation of the tool to the workpiece are ensured with great accuracy by the 7-axis computer-controlled system (Walker et al. 2006). The linear  $X$  ( $Y$ ) axis is mounted to the epoxy granite bridge (base),  $Z$  is mounted on the  $X$  assembly and perpendicular to both  $X$  and  $Y$  and to the turntable surface. The C turntable accepts the workpiece and can rotate it. Tool rotation axes,  $A$ ,  $B$  and  $H$ , are mounted to the  $Z$  assembly.  $H$  spins the tool, which is a rubber membrane of spherical shape, named bonnet. Axes  $A$  and  $B$  intersect  $H$  at the center of curvature of the bonnet called virtual pivot. The sphericity of the bonnet tool and the accuracy of the virtual pivot assembly guarantee the consistency of the contact spot, hence, of the removal rate, throughout the processed surface. As shown in Fig. 2,

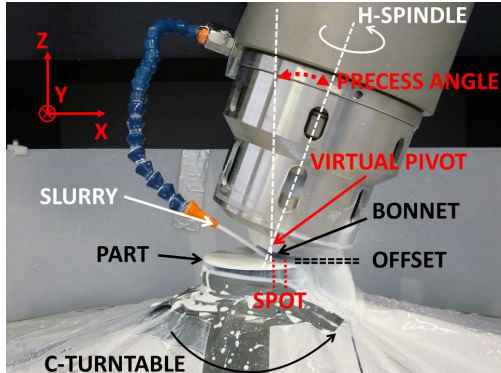


**Fig. 2.** Example of tool-part relative configuration during a polishing run.

the robotic arm is equipped with nozzles delivering the slurry of abrasive particles to the tool-part contact spot.

## 3. Bonnet polishing method

Unlike rigid polishing tools, the bonnet is a compliant tool that conforms well to the local aspheric shape of the surface. The bonnet is inflated by air pressure, typically 1 bar, and covered with some kind of polishing pad such as polyurethane foils. The bonnet-surface distance is preliminarily set to zero by touch, then, the bonnet is advanced towards the surface and compressed against it by an offset of some hundreds of microns to define the contact spot size. In the classical Preston's model for glass polishing (Preston 1927), the material removal rate is proportional to the relative surface speed and to the pressure applied to the part. Surface speed is mostly provided by spinning the tool up to 2000 rounds per minute (rpm). As shown in Fig. 2, the robotic arm is usually set with  $H$  axis inclined as respect to the local normal to the surface. This inclination defines the precess angle, and it is intended to take the zero-velocity pole at the vertex of the bonnet outside the contact spot (Walker et al. 2003). Since tool speed and pressure are usually set constant, the removal at any position depends on the time the tool is remaining there. In the form-correction process, given an error map of the surface, and a set of ma-

chine and process parameters (tool size and speed, offset, precess angle, point spacing), a dwell time map is calculated according to the removal required to correct the measured form error. Finally the machine executes the dwell time map in terms of a varying speed along the tool path. By replacing the bonnet with another of different radius, polishing spots of different size are made available, ranging from few to tens of millimeters. Spots of different size target different intervals of the spatial frequency content that qualifies the error map. The spot with the smallest size roughly sets the highest spatial frequency that is correctable, as the compliance of the bonnet limits its smoothing ability. However, since the removal rate is also decreasing with the spot size, the use of small spots might be impractical, particularly when large optics are involved. The error spatial frequencies not correctable by bonnet can be effectively smoothed out by equipping the robotic arm with tailored pitch tools, as described by Citterio et al. (2011).

#### 4. Fluid jet polishing method

The facility includes the option of Fluid jet as additional polishing method. In this case, the same kind of slurry of abrasive particles is pressurized and projected through a nozzle towards the surface of the workpiece. The SMU is designed to provide pressure stability of  $\pm 0.1$  bar. This feature is aimed particularly to the fluid jet process, where removal rate is directly proportional to the working pressure of the slurry (Fang et al. 2006). Fluid jet is a kinetic machining method, as material is removed by impact of the abrasive particles on the surface. The polishing spot depends on the nozzle geometry and other process parameters, and it is not affected by the edge effect as the bonnet polishing and other contact tool methods (Guo et al. 2006).

#### 5. Results of the acceptance test

Acceptance tests using the bonnet corrective polishing and synchro-spiral techniques have been completed on the machine at our site. The Zeeko bonnet polishing machine pass-off

consists of tests performed on BK7 glass surfaces of two kinds, flat and concave of  $\approx 500$  mm radius, both 100 mm in diameter. Surfaces of quality not yet optical are supplied for testing the synchro-spiral mode. They were previously lapped using 15  $\mu\text{m}$  loose abrasive such that the form error is less than 2  $\mu\text{m}$  Peak-to-Valley (PV). The synchro-spiral mode spins the turntable at a similar speed as the tool, while this is traversing the surface along X or Y direction. This machine's mode performs so-called pre-polishing, that brings the surface from mechanical to optical quality, by removing sub-surface damage and residual marks from previous lapping/grinding processes. Previously pre-polished surfaces are instead taken as starting condition to test the corrective polishing mode. In this case, the tool is rastered along X or Y throughout the surface, at a variable speed accounting for the local dwell-time changes. The requirement to be fulfilled that demonstrates machine's polishing capability consists in a form error reduced to 1/40 wave rms ( $\approx 16$  nm) over the specified clear aperture of 88 mm diameter. The iterative process usually consists of interspersed runs of polishing and metrology (interferometry in this case). Fig. 3 shows that the requirement above has been fulfilled on the concave part by applying two form-corrective runs of  $\approx 190$  min overall time. We used the 20 mm radius bonnet spun at 1400 rpm, 20° precess angle and 0.15 mm offset. The measured initial form error of 786 nm PV and 136 nm rms (left panels of Fig. 3) has been improved to 104 nm PV and 12 nm rms values (right panels), over the 88 mm clear aperture which excludes a contour zone of 5 mm from the chamfered edge. The rate of convergence to the final surface is rather good, and it does arise from the learning curve we had previously followed while correcting the flat surface. In that test we had to modify and optimize the slurry recovery system so as to prevent the slurry settling, e.g., onto the machine's turntable. Otherwise, variations in the slurry's density would cause fluctuations in the removal rate, hence, poor convergence of the process. Therefore, it is important to achieve an accurate knowledge of the removal rate and to keep it stable at most throughout the process.

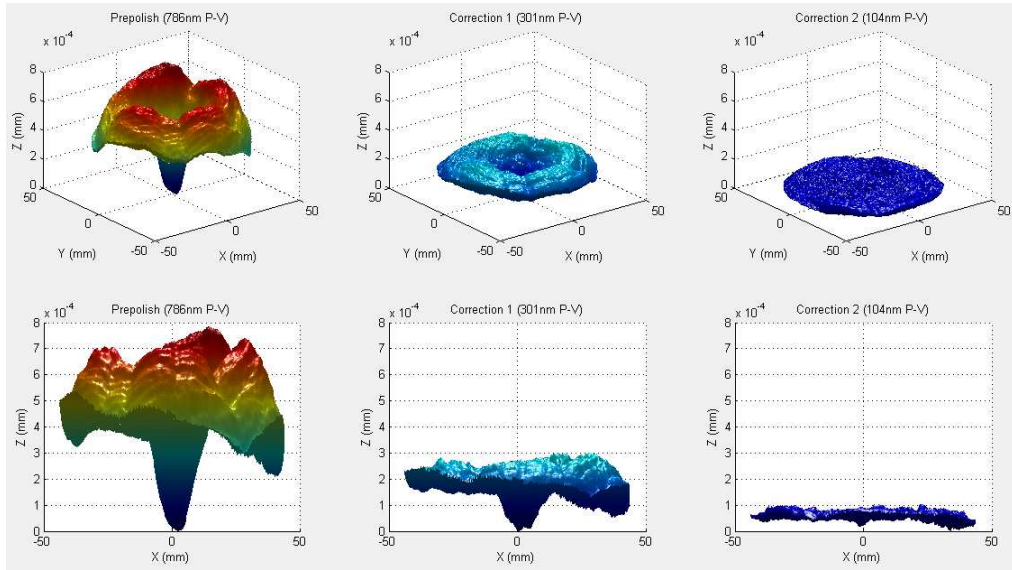


**Fig. 3.** Bonnet polishing machine pass-off test on the 100 mm concave BK7 surface. Top: 3D view of the error map. Bottom: X-Z view. Left: starting condition of the part after pre-polishing (786 nm PV, 136 nm rms). Centre: form error map after the 1<sup>st</sup> corrective run (301 nm PV, 49 nm rms). Right: form error map after the 2<sup>nd</sup> corrective run (104 nm PV, 12 nm rms). [Image courtesy of W. Messelink]

On the flat BK7 surface we achieved an rms value of 19 nm over the 88 mm clear aperture, and 16 nm rms over a slightly reduced clear aperture of 85 mm diameter.

## 6. Conclusions

A Zeeko IRP1200 polishing/forming robotic machine has been implemented within the T-REX project. Machine acceptance test has been completed successfully as of bonnet polishing method. Fluid jet polishing acceptance test is scheduled in short term. The road map of future activity foresees to practicing the most needed processes on test surfaces. On a longer term a large effort will be devoted to the development of the polishing/figuring processes suitable to the production of optical components related to the E-ELT, with particular reference to the optics for the MAORY module. We aim to perform such activity by exploiting the synergy between the two complementary

technologies provided by the IRP1200 and the IBF facility, both available in our labs at INAF-Brera Astronomical Observatory.

## References

- Cayrel, M. 2012, Proc. SPIE, 8444, 84441X
- Citterio, O., et al. 2011, Proc. SPIE, 8147, 814714
- Diolaiti, E., et al. 2014, Proc. SPIE, 9148, 91480Y
- Fang, H., et al. 2003, Appl. Opt., 45, 4012
- Ghigo, M., et al. 2014, Proc. SPIE, 9151, 91510Q
- Guo, P., et al. 2006, Appl. Opt., 45, 6729
- Preston, F. W. 1927, J. Soc. Glass Technol., 11, 247
- Walker, D. D., et al. 2003, Opt. Express, 11, 958
- Walker, D. D., et al. 2006, Proc. SPIE, 6273, 627309